

Estimation of Drain-Induced Barrier Lowering Variation Due to Random Dopant Fluctuation Effect in Nanometer MOSFETs by Gamma Distribution

Weifeng LYU¹, Ying HAN, Caiyun ZHANG, Weijie WEI and Dengke CHEN
Key Laboratory for RF Circuits and Systems of Ministry of Education (Hangzhou Dianzi University), Hangzhou 310018, China

Abstract. Drain-induced barrier lowering (DIBL) and its variations are regarded as significant challenges in nanometer semiconductor device and circuit analysis, design as well as fabrication. This paper investigates the statistical characteristic of DIBL due to random dopant fluctuation (RDF) effect in MOSFETs. The results exhibit that the DIBL variation is more suitably described by a gamma distribution than a Gaussian distribution, based on validation by Monte Carlo simulations. The average error and mean square error of a gamma approximation are -0.14987 and 0.42591, respectively, for the probability density function, and 0.13523 and 0.50584, respectively, for the cumulative density function, which are much smaller than the equivalent measures of a Gaussian approximation. Our study also reveals that DIBL dispersion due to RDF effect in nanometer MOSFET channels is asymmetric with a long tail, which should be described with higher moments such as skewness and kurtosis.

Keywords. Process variations, statistical modeling, nanometer MOSFET, DIBL, RDF effect, gamma distribution

1. Introduction

With the aggressive downscaling of feature sizes, nanometer complementary-metal-oxide-semiconductor (CMOS) integrated devices and circuits encounter many design challenges [1]. More short channel effects (SCEs), especially drain-induced barrier lowering (DIBL), will severely affect device channel barriers and cause transistor performance degeneration, unreliability, and loss of integrated circuit (IC) yield. DIBL referred originally to a reduction of threshold-voltage (V_T) at a higher drain bias voltage (V_d) [2-4]. As an important figure-of-merit (FOM) for ultra-short metal-oxide-semiconductor-field-effect-transistors (MOSFETs), DIBL has attracted great attention in recent years because it drastically influences device drive current as well as gate-to-channel controllability [4]. On the other hand, suppressing DIBL is nearly the most effective way to improve intrinsic gain and output characteristics.

At the same time, process variations (PVs), i.e., the device parameter deviation in MOSFET devices induced by random uncertainty in semiconductor manufacturing, now

¹ Corresponding author: Weifeng Lyu; E-mail: lvwf@hdu.edu.cn

play a crucial role in state-of-the-art CMOS circuit design and fabrication. Moreover, it further has exacerbated the challenge faced by the IC industry as the MOSFETs continuously shrink into the nanometer regime. To overcome these barriers, much effort has been devoted to investigating the impact of various PVs on V_T and/or DIBL [5-7]. Both experimental and theoretical studies have confirmed that V_T and DIBL are very prone to random dopant fluctuation (RDF) effect in nanometer MOSFET channels. As a result, modeling and characterization of DIBL variations associated with RDF effect have attracted much interest for more than a decade [8-10]. For instance, DIBL has been examined against multiple intrinsic variation sources such as RDF, metal gate granularity (MGG), and line edge roughness (LER), and it has been shown that RDF effect causes most of the DIBL variability for planar MOSFETs [6]. Also, the correlation of DIBL with V_T is analyzed in detail with respect to the RDF effect of statistical variability; it reveals that weak correlation between V_T and DIBL results from random discrete charges, but V_T and DIBL are strongly correlated due to random gate-length variation [6]. The clear correlation between negative DIBL and negative differential resistance is observed in negative capacitance MOSFETs [11, 12]. DIBL variability can also significantly affect the static noise margin (SNM) of static random access memory (SRAM) cells; therefore, understanding DIBL and V_T variability will have significant industrial implications. This is because DIBL variation is a critical FOM that determines SNM fluctuation, but the trans-conductance and body factor variation have only a small impact on SNM [6].

From the perspective of statistical distribution modeling, much literature has provided innovative approaches to describe their stochastic behaviors because the accurate prediction of the shape and tail is of great significance for IC fabrication in the presence of variation. On the other hand, an inappropriate prediction in the early design phase such as Gaussian (Normal) approximation will lead to loss of IC yield. Though the Gaussian distribution is very simple with only two moments (mean and variance), and is widely used in IC parameter predictions, it appears increasingly unsuitable to the need of statistical estimation for nanometer MOSFETs and circuit performance. For example, the statistical characteristic of DIBL variation due to position effect of RDF was found to be better described by a lognormal distribution [13]. Device simulations have shown that the RDF-induced V_T distribution in nanometer N-type MOSFET (NMOS) devices deviates from a Gaussian distribution. Some results show that RDF effect has a significant impact on all of the timing parameters of a standard CMOS flip-flop, and these parameters do not follow a Gaussian distribution but are skewed with a large tail, which can better be represented by the Pearson IV system [14]. However, to our best knowledge, there have been only a very few reports considering probability density functions (PDFs) and/or cumulative density functions (CDFs) of DIBL variation due to RDF effect in nanometer MOSFETs, which substantially influences the prediction of stochastic dispersion of device and circuit performance. This paper investigates the statistical characteristic of DIBL due to RDF effect in standard bulk planar-MOSFETs using Monte Carlo simulations. We demonstrate that DIBL variation due to RDF effect can be better characterized by a gamma distribution rather than a Gaussian distribution against the simulation data.

The rest of the paper is organized as follows. Simulation and modeling methodology of DIBL variation for nanometer MOSFETs are discussed in Section II. We emphasize the necessity of a non-Gaussian statistical distribution. The gamma distribution is introduced for estimation of DIBL variation due to RDF effect in Section III. Also, the one-to-one comparison results between gamma and Gaussian approximations are proposed. We have verified that the gamma distribution is more suitable for prediction

of DIBL variation via goodness-of-fit hypothesis tests. Our conclusions are presented in Section IV. Furthermore, we prove that the Pearson IV system is unfit for describing the DIBL variation in due to RDF in the appendix.

2. Device simulation and modeling methodology

The NMOS devices investigated are based on standard planar bulk-CMOS process with state-of-the-art 22-nm technology. The basic device parameters listed in Table.1 are in accordance with Predictive Technology Model (PTM) for low power application. In the study, the numerical experiment is based on the approaches in [8, 9]. Supposing the random variables for the number of dopant atoms are independent with each other, then the dopant atoms in NMOS channel follow Poisson statistical distribution and the standard deviation of them can be analyzed and computed as well. It has to be noted that, to quantify the RDF effect, 3-D Monte-Carlo atomistic TCAD tools based on the finite-element method are necessary to achieve sufficient accuracy. For example, the need of atomistic simulations in the accurate prediction of MOSFET variations with RDF, LER, and WFV has been demonstrated [4, 6]. However, the atomistic simulations are too computationally expensive and time-consuming in device- and circuit-level statistical modeling such as the optimization of SRAM cells [15]. Therefore, an efficient SPICE (PTM) model is much more suitable in some cases. The SPICE model can employ analytical expressions to describe the impact of MOSFET parameters on the electrical performance and through proper parameter extraction, the variation effects can be captured correctly [15, 16]. To correctly capture DIBL variability due to RDF effect, the nanometer MOSFETs studied in this work are also considered with two limit conditions and operation region. Therefore, the simulation results obtained in this work are reasonable and acceptable.

Table 1. Nominal NMOS device parameters

Parameters	values
Effective channel length (L_{eff})	22 nm
Effective channel width (W_{eff})	22 nm
Gate oxide thickness (T_{ox})	1.4 nm
Channel doping concentration (N_{ch})	$5.5 \times 10^{18}/\text{cm}^3$
Source/drain doping concentration ($N_{\text{s/d}}$)	$2.0 \times 10^{20}/\text{cm}^3$
Threshold in linear region ($V_{\text{T,lin}}$)	0.6819V
Threshold in saturation ($V_{\text{T,sat}}$)	0.5687V

The considered DIBL can be analytically expressed as a V_{T} difference with respect to V_{d} . In our work, we extract V_{T} and its small changes with drain bias voltage. Therefore, the computation of $\text{DIBL} = dV_{\text{T}}/dV_{\text{d}}$ with a derivative formula strictly follows this definition. Also, the DIBL variation due to random dopants in MOSFET channels is extracted by Monte Carlo simulations. In our simulations, an ensemble size of 1,000 DIBL samples is randomly reproduced to investigate its statistical characteristics. It has to be noteworthy that we also compared both PDF and CDF of the 1,000 and 10,000 samples from Monte Carlo simulation. It indicates that both of PDF and CDF match very well with the different samples. Therefore, we still use 1,000 samples to capture the statistical characteristics in this work. Figure. 1 shows these DIBL samples together with their nominal value. It is seen from Figure. 1 that the DIBL dispersion does not appear

to be completely symmetric though it fluctuates around its nominal value. Thus, it seems really questionable that the DIBL variation due to RDF effect should be described appropriately by a Gaussian distribution since the Gaussian approximation is only suitable to a symmetric distribution, which is also consistent with existing results [13, 14]. On the other side of the coin, it is fortunate that we realize that the DIBL dispersion might be represented by a gamma statistical approximation. This is because: (1) a gamma distribution can be used to model errors in Poisson regression, and the dopant atoms in a MOSFET channel follow a Poisson distribution; (2) the combination of the Poisson and gamma distributions is a negative binomial distribution, which is widely used in Bayesian statistics and is the conjugate prior for the precision of a Gaussian distribution [17, 18]. In Figure.2, we plot on a normal quantile axis (cumulative probability) to show the curvature together with gamma fit. It can be observed that the gamma fit is better than Normal one. Therefore, gamma distribution seems promising to capture the DIBL variation due to RDF.

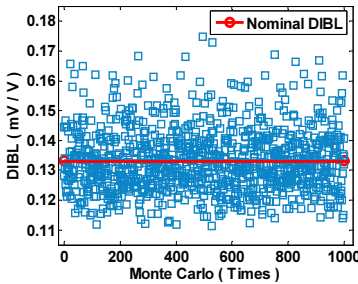


Figure.1 Monte Carlo simulation for DIBL.

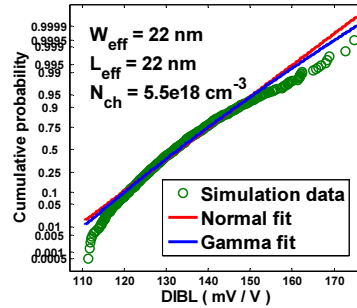


Figure.2 Normal quantile axis with Gamma fit.

3. Results and discussion

To make a fair comparison between Gaussian and gamma approximations for DIBL variation, we first introduce their PDF and CDF expressions in analytical formulas [17-19]:

$$\begin{cases} PDF_{\text{Normal}}(x; \mu, \sigma) = \frac{1}{\sqrt{2\pi}\sigma} \exp\left(-\frac{(x-\mu)^2}{\sigma^2}\right) \\ CDF_{\text{Normal}}(x; \mu, \sigma) = \frac{1}{2} \left[1 + \operatorname{erf}\left(\frac{x-\mu}{\sqrt{2}\sigma}\right) \right] \end{cases} \quad (1)$$

$$\begin{cases} PDF_{\text{Gamma}}(x; \alpha, \beta) = \frac{1}{\beta^\alpha \Gamma(\alpha)} x^{(\alpha-1)} \exp\left(-\frac{x}{\beta}\right) \\ CDF_{\text{Gamma}}(x; \alpha, \beta) = 1 - \frac{1}{\Gamma(\alpha)} \Gamma\left(\alpha, \frac{x}{\beta}\right) \end{cases} \quad (2)$$

where μ and σ are the mean and standard deviation, respectively, fitting parameters α and β denote the shape and scale; $\Gamma(x) = \int_0^{+\infty} t^{x-1} \exp(-t) dt$ and $erf(x) = \frac{2}{\sqrt{\pi}} \int_0^x \exp(-t^2) dt$ are the gamma function and Gaussian error function, respectively. In this study, the parameters $\alpha=165.145$ and $\beta=0.8068$ are extracted by fitting the reproduced samples to the PDF and CDF of a gamma distribution. Figure. 3(a) illustrates the comparison between the proposed gamma distribution and a Normal distribution, together with the reproduced samples in a histogram. It is shown that the DIBL dispersion is asymmetric and slightly skewed. As a result, this kind of distribution cannot be expressed as a normal approximation. Fortunately, it can be matched very well by a gamma distribution. Figure. 3(b) depicts the comparison between the gamma and Gaussian distributions with CDF curves. We can observe that the gamma function matches the simulation data well. The point-to point comparison results of absolute and relative errors are depicted in Figure.4 for both of PDF and CDF. It can be observed that the errors of gamma distribution are generally smaller than the Normal distribution. The statistical analysis for the comparisons is given in Table 2, where MSE denotes the mean square error for the fitting results. From Table 2, we can see that the average errors and MSEs of the gamma approximation are much smaller than those of the Gaussian approximation. The means and MSEs of the gamma approximation are -0.14987 (for PDF), 0.13523 (for CDF), and 0.42591 (for PDF), 0.50584 (for CDF), respectively; however, the average errors and MSEs of the Gaussian approximation are -0.16325 (for PDF), 0.20029 (for CDF), and 0.48443 (for PDF), 0.73449 (for CDF), respectively. So, the gamma distribution achieves greater improvement in mean and MSE as compared to the Gaussian distribution. Therefore, we can say that the gamma distribution is more suitable than the Gaussian distribution for representing the DIBL's statistical characteristics due to RDF. To quantify how well their statistical characteristics represent the sampling data, we can employ goodness-of-fit hypothesis tests [17-21] such as the χ^2 , Kolmogorov-Smirnov (K-S) and rank sum (R-S) tests. The χ^2 test [19] compared the observed histogram measures and the expected probability distribution using a normalized difference for the measured points:

$$\chi^2 = \sum_{i=1}^n \frac{(O_i - E_i)^2}{E_i} \tag{3}$$

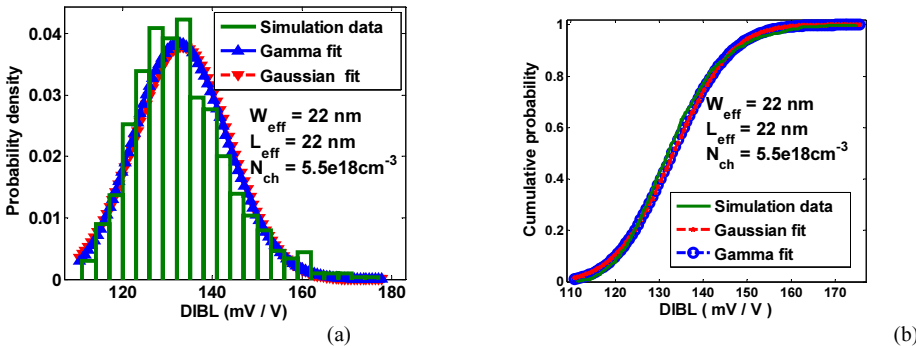


Figure.3 DIBL variation using gamma and Gaussian approximations with simulation data. (a) PDF approximation. (b) CDF approximation.

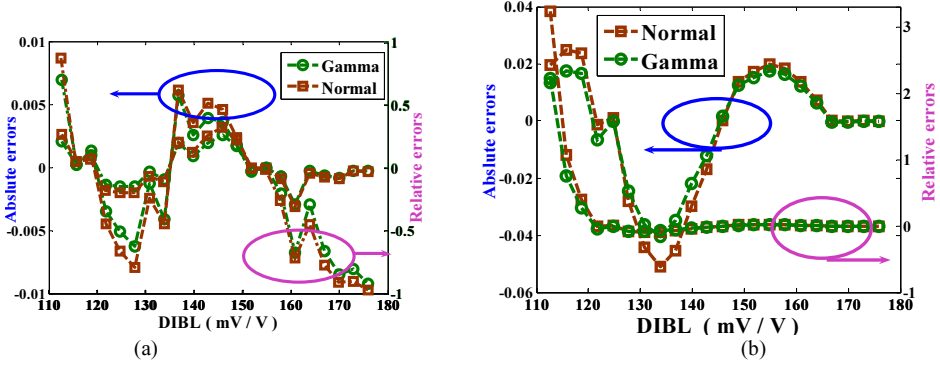


Figure. 4 Error comparisons of Gamma and normal approximations. (a) PDF. (b) CDF.

A larger value of χ^2 indicates a greater difference between the observed and expected data. The K-S test can be used to test whether two underlying one-dimensional probability distributions differ, and it checks whether the two data samples come from the same distribution. The K-S statistic is expressed as

$$D = \sup_x |F(x) - H(x)| \quad (4)$$

where $F(x)$ and $H(x)$ are the empirical distribution functions of the first and second reproduced samples, respectively, and \sup is the supremum function. The R-S test is a nonparametric statistical hypothesis test used to test whether the population mean ranks of two samples differ. It can be used when the population cannot be assumed to be Gaussian. This test calculates the statistic W as the sum of the signed ranks:

$$W = \sum_{i=1}^{M_r} [\text{sgn}(x_{2,i} - x_{1,i}) \times R_i] \quad (5)$$

where sgn denotes the sign function, R_i is the rank. W follows a specific distribution, which is with an expected value of 0 and a standard deviation of $\sqrt{\frac{1}{6} M_r \times (M_r + 1) \times (2M_r + 1)}$. W can be compared to a critical value from a reference table.

For any hypothesis tests, there will be a corresponding p -value ($0 < p < 1$) representing the probability that the dataset follows the presented distribution [18-20]. The greater the p -value, the better the fitting result. A χ^2 test of the fitting data for frequency of occurrence shows that the gamma distribution (p -value 0.1136) fits the observed samples much better than the results reproduced by a normal distribution (p -value 0.00346). Thus, the p -value indicates that only the gamma distribution is above the lower bound (confidence probability 0.05), representing the simulation samples. A K-S test for the ensemble of 1,000 samples data points presented in Figure. 1 and Figure. 3 shows that the gamma distribution matches better than the normal distribution. Also, an R-S test for the dataset indicates that the gamma distribution is more suitable than a normal distribution. Therefore, it is reasonable to assume that a gamma distribution more accurately represents the observed samples from the Monte Carlo simulations than does a Gaussian distribution.

Table 2. Statistics of error for Gaussian and Gamma approximations

Statistics		Gaussian		Gamma		Improvement (%)	
		PDF	CDF	PDF	CDF	PDF	CDF
mean	Absolute	-0.0003186	-0.0026522	-0.0002403	-0.0022228	32.5843	19.3180
	Relative	-1.1632464	0.20028982	-0.1498741	0.13522862	8.92236	48.1120
MSE	Absolute	0.00354896	0.02300587	0.0028836	0.0182769	23.0739	25.8740
	Relative	0.48442704	0.73449084	0.4259140	0.5058376	13.7382	45.2029

The statistically significant moments for each distribution are given in Table 3 with maximum-log likelihood, which is numerically computed from the fitting results, requiring one to minimize the negative log likelihood [19]. It is observed that with the proposed gamma distribution, the statistical dispersion of DIBL variation with non-normal tail can be extracted from the data ensemble. This can be explained by the fact that the gamma distribution can correctly capture the skewness of DIBL dispersion. On the contrary, it is clearly known that the Gaussian distribution cannot describe the asymmetric long tail statistical characteristic. It is also worth noting that the skewness and dispersion of the device and/or circuit parameters will increase with CMOS technology scaling. So, the study of the exact shape of parameter distributions, especially in the tail region, will be of fundamental importance in the prediction of high-performance, highly reliable, and feasible nanometer devices and circuits [15]. As a result, non-Gaussian statistical distributions will play an essential role in estimating IC performance and yield for state-of-the-art nanometer technology. Some variations in device parameters (V_T) and/or circuit parameters (timing) due to RDF effect follow a Pearson IV distribution [15]. However, we prove that the samples reproduced by Monte Carlo simulations cannot support that the suitability of the Pearson IV system to represent DIBL variation if we use the moments' method proposed in.

Table 3. Moments of gaussian and gamma approximations with simulation.

Statistical moments	Gamma	Gaussian	Simulation
Mean, μ (mV)	133.245	133.245	133.245
Standard deviation, σ (mV)	10.3686	10.5237	10.5237
Skewness	0.1556	0	0.7141
Kurtosis	3.03633	3	3.6430
Log likelihood	-3755.69	-3772.07	/

4. Conclusion

We have proposed an investigation of DIBL variation of nanometer bulk-MOSFET devices due to RDF effect via Monte Carlo simulations. Our investigation indicates that RDF effect has significant impact on the DIBL performance. Though the utilization of Gaussian distributions to estimate parameter variation is common in IC design, the statistical characteristics of the parameters of interest perhaps deviate drastically from a Gaussian one. We also have demonstrated that DIBL variation due to RDF effect can be characterized by a gamma distribution via validation against the simulation data. As shown in Table 2, the gamma distribution has great improvement in mean (48.112%) and MSE (45.2029%) as compared to the Gaussian distribution. Thus, the estimation of

DIBL variation provided by the gamma distribution is more accurate compared with the Gaussian distribution. Furthermore, it has been shown that the DIBL distribution has higher moments such as skewness and kurtosis, which will increase with technology scaling. Therefore, the accurate estimation of the shape and tail is of great importance for improving performance and yield of IC designs in the presence of variation.

Acknowledgments

This work is supported by National Natural Science Foundation of China (grant 62071160), and Zhejiang Provincial Natural Science Foundation of China (grant LY22F040001).

References

- [1] Markov IL. Limits on fundamental limits to computation. *Nature*. 2014 Aug; 512(7513): 147-154.
- [2] Yu T, Lü W, Zhao Z, Si P. Negative drain-induced barrier lowering and negative differential resistance effects in negative-capacitance transistors. *Microelectronics Journal*. 2021 Feb; 108: 104981.
- [3] Huang W, Zhu H, Zhang Y, Wu Z, Jia K, Yin X, Li Y, Li C, Ai X, Huo Q, Li J. Investigation of negative DIBL effect for ferroelectric-based FETs to improve MOSFETs and CMOS circuits. *Microelectronics Journal*. 2021 Aug; 114: 105110.
- [4] Hung Y, Chang T, Tu Y, Lu I, Zheng Y, Chiang C, Chen J, Kuo C, Sun L, Zhou K. Improving drain-induced barrier lowering effect and hot carrier reliability with terminal via structure on half-corbino organic thin-film transistors. *IEEE Electron Device Letter*. 2022 Feb;43(4): 569-72.
- [5] Liu B, Chen X, Xie Z, Guo M, Zhao M, Lü W. Reduction of Random Dopant Fluctuation-induced Variation in Junctionless FinFETs via Negative Capacitance Effect. *Informacije MIDEM*, 2021 Dec; 51(4): 253-259, 2021.
- [6] Wang X, Brown A R, Cheng B, Roy S, Asenov A. Drain bias effects on statistical variability and reliability and related subthreshold variability in 20-nm bulk planar MOSFETs. *Solid-state Electronics*. 2014 Aug; 98: 99-105.
- [7] Jiang X, Guo S, Wang R, Cheng B, Asenov A, Huang R. A device-level characterization approach to quantify the impacts of different random variation sources in FinFET technology. *IEEE Electron Device Letters*. 2016 Aug; 37(8): 962-65.
- [8] Lü W, Sun L I. Compact modeling of response time and random-dopant-fluctuation-induced variability in nanoscale CMOS inverter. *Microelectronics Journal*. 2014 Jun; 45(6): 678-82.
- [9] Lü W, Wang G, Sun L. Analytical modeling of cutoff frequency variability reserving correlations due to random dopant fluctuation in nanometer MOSFETs. *Solid-State Electronics*. 2015 Mar; 105: 63-69.
- [10] Tsutsumi T, Lee J. Study of threshold voltage fluctuation caused by source and drain extensions doping variation of tri-gate fin-type FET using three-dimensional device simulation. *Japanese Journal of Applied Physics*. 2014 May; 53(6S): 06JE06.
- [11] Lü W, Chen X, Liu B, Xie Z, Zhao M. Comprehensive performance enhancement of a negative-capacitance nanosheet field-effect transistor with a steep sub-threshold swing at the sub-5-nm node. *Microelectronics Journal*. 2022 Feb; 120: 105363.
- [12] Guo M, Lü W, Zhao M, Xie Z. Effect of the Single-and Dual-k Spacers on a Negative-capacitance Fin Field-effect Transistor. *Silicon*. 2022 Mar; 14(16): 10827-10835.
- [13] Damrongplisit N, Zamudio L, Liu T J K, Balasubramanian S. Threshold voltage and DIBL variability modeling based on forward and reverse measurements for SRAM and analog MOSFETs. *IEEE Transactions on Electron Devices*. 2015 Apr; 62(4): 1119-1126.
- [14] Vanderbauwhede W, Rodríguez-Salazar F. Impact of random dopant fluctuations on the timing characteristics of flip-flops. *IEEE Transactions on Very Large Scale Integration (VLSI) Systems*. 2010 Nov; 20(1): 157-161.
- [15] Lu D, Lin C, Niknejad A, Hu C. Compact modeling of variation in FinFET SRAM cells. *IEEE Design & Test of Computers*. 2010 Mar; 27(2): 44-50.
- [16] Ye Y, Liu F, Chen M, Nassif S, Cao Y. Statistical modeling and simulation of threshold variation under random dopant fluctuations and line-edge roughness. *IEEE Transactions on Very Large Scale Integration (VLSI) Systems*. 2010 Jul; 19(6): 987-996.

- [17] Moschopoulos P G. The distribution of the sum of independent gamma random variables. *Annals of the Institute of Statistical Mathematics*. 1985 Dec; 37(1): 541-544.
- [18] Bevington P, Robinson D, Blair J, et al. Data reduction and error analysis for the physical sciences. *Computers in Physics*. 1993; 7(4): 415-416.
- [19] Indalecio G, Garcia-Loureiro A, Iglesias N, Kalna K. Study of metal-gate work-function variation using Voronoi cells: comparison of rayleigh and gamma distributions. *IEEE Transactions on Electron Devices*. 2016 Jun; 63(6): 2625-2628.
- [20] Hu D, Yu X, Wang J. Statistical inference in rough set theory based on Kolmogorov–Smirnov goodness-of-fit test. *IEEE Transactions on Fuzzy Systems*. 2016 Jun; 25(4): 799-812.
- [21] Heinrich J. A guide to the Pearson type IV distribution. University of Pennsylvania. 2004 Dec; 1-2.